

# Hierarchical Latent Class Models for Mortality Surveillance Using Partially Verified Verbal Autopsies

Yu Zhu<sup>1</sup> and Zehang Richard Li<sup>1</sup>

<sup>1</sup>Department of Statistics, University of California, Santa Cruz

## Abstract

Monitoring data on causes of death is an important part of understanding the burden of diseases and effects of public health interventions. Verbal autopsy (VA) is a well-established method for gathering information about deaths outside of hospitals by conducting an interview to family members or caregivers of a deceased person. Existing cause-of-death assignment algorithms using VA data require either domain knowledge about the symptom-cause relationship, or large training datasets. When a new disease emerges, however, only limited information on symptom-cause relationship exists and training data are usually lacking, making it challenging to evaluate the impact of the disease. In this paper, we propose a novel Bayesian framework to estimate the fraction of deaths due to an emerging disease using VAs collected with partially verified cause of death. We use a latent class model to capture the distribution of symptoms and their dependence in a parsimonious way. We discuss potential sources of bias that may occur due to the cause-of-death verification process and adapt our framework to account for the verification mechanism. We also develop structured priors to improve prevalence estimation for sub-populations. We demonstrate the performance of our model using a mortality surveillance dataset that includes suspected COVID-19 related deaths in Brazil in 2021.

*Keywords:* Verification bias; structured prior; domain adaptation; semi-supervised learning.

# 1 Introduction

Monitoring data describing cause of death is an essential component for understanding the burden of disease and evaluating public health interventions. Only about two-thirds of deaths worldwide are registered and up to half of these deaths do not have an assigned cause, with the least information available from countries with the most need (World Health Organization, 2021). A widely used tool to obtain information on causes of death when a medically certified cause-of-death is not available is verbal autopsies (VA). VA involves a structured questionnaire administered to family members or caregivers of a recently deceased person. The VA interviews collect information about the circumstances, signs, and symptoms leading up to death. VAs are widely adopted both in research settings and by national statistical offices (e.g., Maher et al., 2010; Nkengasong et al., 2020). Such information is either analyzed by physicians or with statistical algorithms to assign causes of death.

During public health emergencies when a new disease emerges, VA is usually the only feasible tool to gather information on causes of death in many low-resource settings, e.g., during the Ebola hemorrhagic fever outbreaks (Alert et al., 2003), the Dengue epidemic (Saqib et al., 2014), and the COVID-19 pandemic (de Souza et al., 2020; Rosen et al., 2021). In such settings, physician review of VAs is usually infeasible since the process is time-consuming and expensive, especially during a public health crisis, and cause-of-death assignment needs to be performed by automatic VA algorithms in any medium- to large-scale mortality surveillance settings.

While significant advances have been made in automatic cause-of-death assignment algorithms in the last several decades (Chandramohan et al., 2021), using VAs for the purpose of

monitoring mortality patterns and trends due to a new disease remains challenging. First, all existing VA algorithms operate with a pre-defined set of symptoms and causes and their relationships are either provided by physicians and assumed to be known (Byass et al., 2019; McCormick et al., 2016) or need to be estimated from high-quality training data, i.e., reference deaths with known causes verified through a separate mechanism (Kunihama et al., 2020; Moran et al., 2021). In the case of a new disease, the relationship between symptoms and the new cause of death is generally unknown and needs to be estimated from the limited training data, i.e., reference deaths with verified cause of death, during the outbreak. Moreover, the subset of deaths with the cause of death verified may not be a random sample of the target population, due to logistical reasons and changing public health priorities. Such reference deaths can exhibit different symptom-cause relationships and VA algorithms trained on these deaths could lead to biased estimates if the selective sampling process is not properly accounted for. This issue is similar to the verification bias in the diagnostic test literature, where the accuracy of a diagnostic test can be distorted by evaluation based on the patients with verified disease status only (Zhou, 1998). To our knowledge, there are no guidelines or recommendations in the literature to account for the selection process of reference death in VA research.

Second, the target of inference for mortality surveillance is usually the time-varying prevalence of the disease, potentially further stratified by key demographic groups. Existing literature on VA analysis, however, typically focuses on estimating the cause-specific mortality fraction (CSMF) for a single target population with a stable distribution of symptoms and causes of death. During the course of an outbreak, the population mortality profiles can change rapidly, due to both disease dynamics and changing treatment and intervention

measures. Thus the accuracy of cause-of-death assignment methods trained on data from the early phase of an outbreak may deteriorate over time. Therefore, it is important to flexibly adapt the model to the changing distribution over time and across related sub-populations. A related line of work by Moran et al. (2021) and Kuniyama et al. (2024) shows that modeling covariate-dependent symptom distributions can improve VA algorithms in general. However, their target of inference is still the overall prevalence of a static population, instead of time-varying or sub-population prevalence. As we demonstrate in both simulation and real data analysis, directly extending single-population models by treating the sub-populations as independent can lead to estimates with large variations, especially when the sample size is small.

Both challenges are closely related to the generalizability of VA algorithms from a non-representative training dataset to one or multiple target populations. In this paper, we address these two issues in a unified framework by extending the models in Li et al. (2024) and Wu et al. (2024) to a hierarchical framework to deal with the distribution shift across multiple sub-populations. We focus on estimating the prevalence of a single disease over time for sub-populations defined by key demographic indicators. We propose a hierarchical latent class model informed by the causal structure of the cause verification process to account for the heterogeneity of the collected data stream. Furthermore, we propose a novel set of structured priors on the sub-population prevalence to efficiently borrow information and improve the precision of estimates.

The rest of the paper is organized as follows. Section 2 introduces our proposed nested latent class model with structured priors over sub-populations. Section 3 develops an efficient Markov Chain Monte Carlo (MCMC) algorithm for posterior sampling. Section 4

demonstrates the proposed model with a series of simulation experiments and a COVID-19 surveillance dataset from Brazil. Section 5 concludes with a discussion of limitations and future work on using VA for mortality surveillance.

## 2 Models

### 2.1 Verification mechanism

Let  $X_i \in \{0, 1\}^p$  denote the  $p$ -dimensional vector of signs/symptoms for the  $i$ -th death and  $Y_i \in \{0, 1\}$  denote the corresponding cause of death. The overall prevalence of the disease is  $p(Y)$ . We consider the case where only a subset of deaths were verified, i.e., assigned a cause by an independent mechanism. Let  $L_i \in \{0, 1\}$  be the indicator of whether the cause of death for the  $i$ -th death is known. We refer to the process generating  $L$  as the verification mechanism thereafter. Existing literature typically assumes that  $L_i = 1$  for all deaths with VAs in some training populations, usually different from the target population where cause-of-death assignment is performed, and various assumptions between the training and target distributions are made to ensure transportability of the classifier (Li et al., 2024). Here we focus on a different scenario where a subset of the deaths in the target population have a known cause-of-death label  $L$ .

When the verified deaths, i.e., the training data, are a subset of the target population, it becomes crucial to understand how the deaths are selected for verification. If the training subset is not a simple random sample of the population, models estimated using the verified deaths may be inadequate to generalize to the entire population directly. In surveillance

settings, it is common to over-sample deaths of certain characteristics, e.g., deaths in certain age groups or from certain locations, into the verification dataset in order to increase the chance of identifying certain deaths, and the selection process may also change over time. Valid inference is still possible if the verification mechanism is conditionally ignorable, i.e., it depends only on the observed quantities. Assumption 1 formally characterizes such scenarios.

**Assumption 1** *The selection probability of receiving a verified cause of death only depends on known stratification variables  $D$  and symptoms  $X$ , but not the cause of death  $Y$  or other unobserved variables associated with  $Y$ . That is,  $L \perp Y \mid X, D$ .*

Assumption 1 is equivalent to assuming that the cause of death is missing at random (Rubin, 1976). The choice of  $D$  should be informed by how the reference deaths with verified causes are selected. When selection probability depends on known and observable variables, we can let  $D$  be the strata defined by these variables. When the verification mechanism is not clearly specified, the choice of  $D$  is contextual. Including more covariates in  $D$  mitigates the bias from potential violation of the conditional ignorability assumption but it increases model complexity. In practice, proxy variables such as time period and region indicators may be included in  $D$  to mitigate the effect from any unobserved variables that vary over time or space.

## 2.2 Semi-supervised approach

Given a choice of  $D$  that renders the selection mechanism conditionally ignorable, it suffices to learn a binary classification rule using the training dataset. The population prevalence can be estimated by  $\hat{p}(Y) = \frac{1}{n} \sum_{i=1}^n \hat{p}(Y \mid X = x_i, D = d_i, L = 1)$ . Sub-population prevalence

$p(Y | D = d)$  can also be obtained by aggregation in a similar fashion. A major drawback of such discriminant classification models, however, is that they do not take into account the potentially large collection of unlabelled VA data. On the other hand, semi-supervised approaches that model both the labelled and unlabelled data can achieve better predictive performance in tasks where  $Y$  is the ‘cause’ of the observed covariates  $X$ , as the distribution of  $X$  in the unlabelled data also contains information about the conditional distribution of  $X$  given  $Y$  (Kügelgen et al., 2020). Classification tasks with this type of structure are usually referred to as being ‘anticausal’ (Schölkopf et al., 2012). The VA problem is anticausal in nature because the majority of the symptoms and indicators are consequences of the underlying cause of death (King and Lu, 2008; Li et al., 2024). Figure 1a illustrates the data generating process of the observable quantities under the assumed anticausal structure and the conditional independence relationship in Assumption 1. Therefore, in this work, we treat the unknown cause of death  $Y$  as missing data and fit our models on all the deaths together.



(a) Ignorable verification given stratum  $D$  and (b) Ignorable verification given stratum  $D$ , covariate  $X_C$  and symptoms  $X_E$ .

Figure 1: Directed acyclic graph (DAG) describing different data generating processes and sample selection mechanisms.  $D$  and  $X_C$  are observed for all deaths and  $Y$  is only observed when  $L = 1$ .

It is also worth noting that the targets of inference may depend on the stratification of the

population by variables collected by the VA survey itself, such as sex and age of the deceased. Strictly speaking, the graphical model in Figure 1a can be refined by further partitioning the variables collected by VA into  $X = (X_C, X_E)$  where  $X_C$  are variables that affect the risk of the cause of death, e.g., demographic variables, and  $X_E$  are the variables affected by the cause of death, e.g., medical symptoms. This leads to the data generating process shown in Figure 1b. Previous work on VA models typically do not differentiate  $X_C$  from  $X_E$ . The only two exceptions in the literature are Moran et al. (2021) and Kuniyama et al. (2024). Both papers consider separating some covariates from the rest of the symptoms, and model the conditional distribution of covariates given cause of death. They have shown that explicit estimation of symptom distribution given covariates improves the estimation of the prevalence under latent Gaussian factor models. They aim to flexibly characterize the joint distribution of symptoms. Our motivation is different. We choose  $X_C$  to be the pre-disease variables that define meaningful strata in the population, and our target of inference is the sub-population prevalence  $p(Y | D, X_C)$  instead of  $p(Y)$ . Therefore, instead of modeling the conditional distribution of covariates given cause of death as in previous work, we explicitly model the conditional distribution of cause of death given covariates  $X_C$ . This factorization also enables the use of more interpretable and structured prior specification for  $p(Y | D, X_C)$  described in Section 2.4. To simplify notation in the rest of the paper, we omit  $X_C$  and  $X_E$ , and use  $D$  to denote any variables defining stratification regardless of whether they are collected in the VA survey, and  $X$  to denote the rest of the indicators from the VA survey.



## 2.3 Nested latent class model

We now turn to model specification. Let  $D_i \in \{1, \dots, G\}$  denote the combination of all levels of the stratification variables. The anticausal structure in Figure 1 leads to the factorization of the joint distribution  $p(X, Y, D) = p(D)p(Y | D)p(X | Y, D)$ . Many existing VA models simplify the last conditional probability into  $p(X | Y)$  by assuming the conditional distribution of symptoms are transferable (e.g., McCormick et al., 2016; Byass et al., 2019). Such assumptions are usually violated when considering symptom distributions across deaths of different sex and age groups (Moran et al., 2021) or over different populations (Li et al., 2024). To illustrate the conditional dependence on  $D$ , we use the COVID-19 dataset described in Section 4.2 to compute the empirical symptom prevalence and the Matthews correlation coefficient (Matthews, 1975) of some selected symptoms across different age groups and over time. Figure 2 shows that the symptom prevalence varies across both time and age groups. For example, among COVID-19 related deaths, the proportion of observations with fever as a symptom decreases over time and as age increases. Figure 3 shows that the dependence among symptoms also varies significantly with the age and time period of the death.

In order to capture the heterogeneity of symptoms distributions over different subpopulations in a parsimonious way, we adopt the nested latent class model framework proposed in Li et al. (2024) and Wu et al. (2024), where individual-level latent class membership indicator  $Z_i \in \{1, 2, \dots, K\}$  is introduced to flexibly capture the dependence of  $X$ . We assume

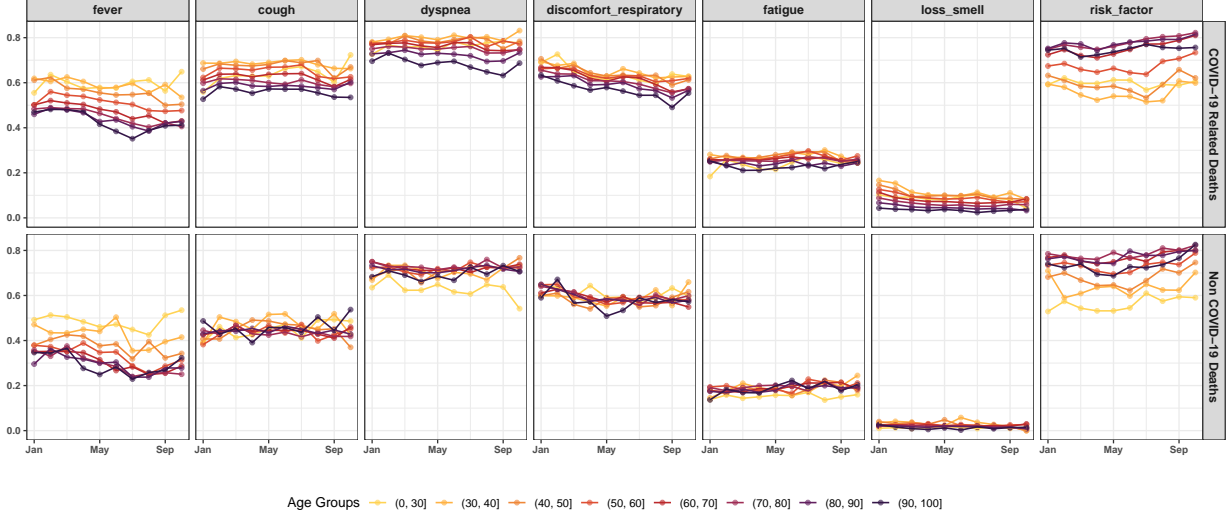


Figure 2: Time-varying proportion of deaths reporting different symptoms across eight age groups and two causes of death, among deaths the Brazil VA dataset.

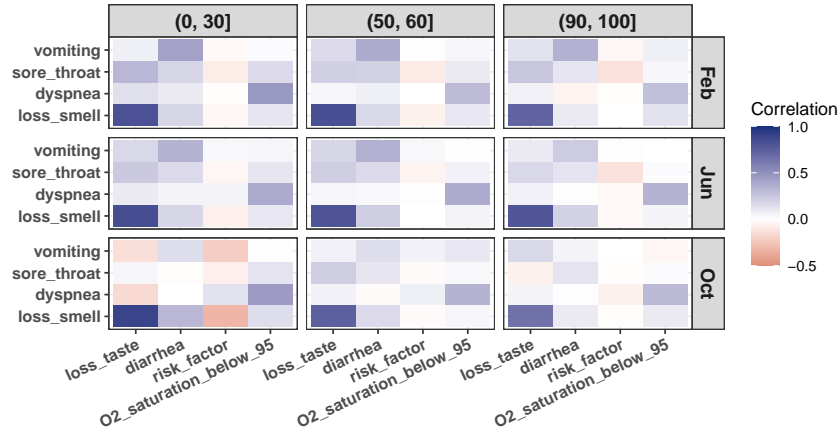


Figure 3: Matthews correlation coefficient (Matthews, 1975) of a subset of symptoms among deaths related to COVID-19 among deaths in three age groups from three time periods in the Brazil VA dataset. Missing data are removed in calculating correlation coefficient.

the following data generating process,

$$Y_i \mid D_i = g \sim \text{Bern}(\pi^{(g)}), \quad (1)$$

$$Z_i \mid Y_i = c, D_i = g \sim \text{Cat}(\boldsymbol{\lambda}_c^{(g)}), \quad (2)$$

$$X_{ij} \mid Y_i = c, Z_i = k \sim \text{Bern}(\phi_{ckj}), \quad j = 1, \dots, p. \quad (3)$$

The introduction of the latent class nested under each cause of death leads to a flexible characterization of cause-specific dependent symptom profiles that vary across strata, i.e., after integrating out the latent indicators, the conditional distribution of symptoms given a cause of death and sub-population is  $p(X_i | Y_i = c, D_i = g) = \sum_k \lambda_{ck}^{(g)} \prod_j \phi_{ckj}^{x_{ij}} (1 - \phi_{ckj})^{1-x_{ij}}$ . When  $K = 1$ , the model reduces to the commonly used conditional independent model in McCormick et al. (2016). In order to facilitate easier interpretations and mitigate the risk of overfitting, we fix the latent response probabilities  $\phi$  to be invariant across strata and let the sub-populations mix differently over the latent symptom profiles. With sufficiently many latent classes  $K$ , this representation is flexible enough to capture any multivariate discrete distribution (Dunson and Xing, 2009).

The prior specification of  $\pi^{(g)}$  needs to be designed for the specific choice of stratification variable  $D$ . We discuss our structured prior for  $\pi^{(g)}$  in the next subsection. For the rest of the latent parameters, we put stick-breaking priors on  $\lambda_c^{(g)}$  and conjugate Beta priors on  $\phi$ , i.e.,

$$\lambda_{ck}^{(g)} = V_{ck}^{(g)} \prod_{l < k} (1 - V_{cl}^{(g)}), \quad V_{ck}^{(g)} \sim \text{Beta}(1, \omega_c^{(g)}), \quad \text{for } k = 2, \dots, K,$$

$$V_{cK}^{(g)} = 1, \quad \omega_c^{(g)} \sim \text{Gamma}(a_\omega, b_\omega), \quad \phi_{ckj} \sim \text{Beta}(a_\phi, b_\phi).$$

We treat any unknown  $Y_i$  as missing data without modeling the verification process due to Assumption 1. Missing values in the symptoms are also common in practice. We follow the practice of current VA algorithms by assuming they are also missing at random (Kunihama et al., 2020).

## 2.4 Stratification and structured priors

A main challenge when considering fine stratification of a population is that inevitably some sub-populations will contain only a small number of deaths. Previous work involving cause-of-death assignment in multiple populations all assume independent priors for  $\pi^{(g)}$  (see e.g., McCormick et al., 2016; Li et al., 2024; Wu et al., 2024). For mortality monitoring of small sub-populations, however, it is usually more appropriate to borrow information across related sub-populations in order to improve the stability and interpretability of estimated prevalence. Similar ideas have been extensively studied for survey data in the context of small area estimation (e.g., Rao and Molina, 2015; Gao et al., 2021), but it has not been explored in VA analysis. Unlike the traditional small area estimation literature, the main target of interest in VA analysis, the cause of death, cannot be directly collected and needs to be estimated instead. Nevertheless, we adopt similar ideas to leverage the structured relationship of sub-populations and directly borrow information across strata.

To fix notation, here we consider sub-populations defined by three stratification variables. Let  $S_i \in \{1, 2\}$  indicate sex (1 = female and 2 = male),  $T_i \in \{1, 2, \dots, T\}$  indicate the time period and  $A_i = \{1, 2, \dots, A\}$  indicate the age group of the  $i$ -th death respectively. We reparameterize the nested latent class model with

$$p(Y_i = 1) = \pi_{s[i],t[i],a[i]}, \tag{4}$$

$$p(Z_i = k \mid Y_i = c) = \lambda_{ck}^{(s[i],t[i],a[i])}. \tag{5}$$

We can then encode different prior beliefs into the prior distributions for  $\boldsymbol{\pi}$ . In this paper,

we consider a linear model on the logit scale,

$$\pi_{sta} = \text{logit}^{-1}(\mu + \alpha^{\text{male}} \mathbb{1}_{s=1} + \alpha_t^{\text{time}} + \alpha_a^{\text{age}} + \epsilon_{sta}). \quad (6)$$

We model  $\mu$  and  $\alpha^{\text{male}}$  as fixed effects with independent  $N(0, 100)$  priors. For the time and age effects, We consider the following three prior specifications:

1. Fixed effect:  $\alpha_t^{\text{time}} \sim N(0, 100)$  and  $\alpha_a^{\text{age}} \sim N(0, 100)$ .
2. Independent random effect:  $\alpha_t^{\text{time}} \sim N(0, \sigma_{\text{time}}^2)$  and  $\alpha_a^{\text{age}} \sim N(0, \sigma_{\text{age}}^2)$ ,
3. First order random walk (RW1):  $\alpha_t^{\text{time}} \mid \alpha_{t-1}^{\text{time}} \sim N(\alpha_{t-1}^{\text{time}}, \sigma_{\text{time}}^2)$  and  $\alpha_a^{\text{age}} \mid \alpha_{a-1}^{\text{age}} \sim N(\alpha_{a-1}^{\text{age}}, \sigma_{\text{age}}^2)$  for  $t = 2, \dots, T$  and  $a = 2, \dots, A$ .  $\alpha_1^{\text{time}} \sim N(0, 100)$  and  $\alpha_1^{\text{age}} \sim N(0, 100)$ .

For the hyperpriors, we use  $\text{Inv-Gamma}(0.5, 0.0015)$  prior for the variance parameters of independent random effects and  $\text{Inv-Gamma}(0.5, 0.0009)$  prior for the random walk models. These prior choices lead to a 95% prior interval of  $(0.5, 2)$  for the residual odds ratio (Mercer et al., 2015). Finally, we let  $\epsilon_{sta} \stackrel{iid}{\sim} N(0, \sigma_\epsilon^2)$  be an unstructured interaction term that captures the deviation from the main additive decomposition, with hyperprior  $\sigma_\epsilon^2 \sim \text{Inv-Gamma}(0.5, 0.0015)$ .

The three prior specifications differ in the amount of information shared across strata. In the fixed effect model, no information is shared except for the additive structure of the time and age effect. The independent random effect model further shrinks these effects to the common mean. The random walk model shrinks these effects so strata with similar ages or time periods will have similar prevalence.

To assess the benefits of incorporating structured priors, we also compare the three models above with an unstructured baseline model, where  $\pi_{sta} \stackrel{iid}{\sim} \text{Beta}(1, 1)$ . This serves as a benchmark for evaluating the impact of the structured priors on the model’s performance. The unstructured prior is the standard practice in the literature and practice of VA analysis (McCormick et al., 2016; Li et al., 2023). Lastly, when the target of inference is only the overall prevalence, one may consider an unstratified baseline model, where  $\pi_{sta} = \pi_0 \sim \text{Beta}(1, 1)$  for all strata. As we have discussed in Section 2.1, this unstratified model can lead to biased prevalence estimates if the verification mechanism changes over variables not accounted for by the model (e.g., time period). We will demonstrate such bias in simulation and real data analysis in Section 4.2.

### 3 Posterior inference

The posterior distribution of the model parameters is not available in closed form, but we can easily obtain posterior samples from a Gibbs sampler as follows.

1. Sample  $Y_i \mid \mathbf{X}_i, \boldsymbol{\pi}, \boldsymbol{\phi}, \boldsymbol{\lambda}$  for  $i$  where  $L_i = 0$  with

$$p(Y_i = c \mid \mathbf{X}_i, \boldsymbol{\pi}, \boldsymbol{\phi}, \boldsymbol{\lambda}) \propto \pi_{s[i],t[i],a[i]}^c (1 - \pi_{s[i],t[i],a[i]})^{1-c} \sum_{k=1}^K \lambda_{ck}^{(s[i],t[i],a[i])} \prod_{j=1}^p \phi_{ckj}^{X_{ij}} (1 - \phi_{ckj})^{1-X_{ij}}.$$

2. Sample  $Z_i \mid Y_i = c, \mathbf{X}_i, \boldsymbol{\phi}, \boldsymbol{\lambda}$  for  $i = 1, \dots, n$  with

$$p(Z_i = k \mid Y_i = c, \mathbf{X}_i, \boldsymbol{\phi}, \boldsymbol{\lambda}) \propto \lambda_{ck}^{([s[i],t[i],a[i])} \prod_{j=1}^p \phi_{ckj}^{X_{ij}} (1 - \phi_{ckj})^{1-X_{ij}}.$$

3. Sample  $\boldsymbol{\pi} \mid \mathbf{Y}$  with Pólya-Gamma augmentation. Let  $m^{(s,t,a)} = \text{logit}(\pi^{(s,t,a)})$  and rewrite the model as  $\mathbf{m} = \mathbf{P}\boldsymbol{\eta}$ , where  $\mathbf{P}$  is the known design matrix and

$$\boldsymbol{\eta} = \left( \mu, \alpha^{\text{male}}, \alpha_1^{\text{time}}, \dots, \alpha_T^{\text{time}}, \alpha_1^{\text{age}}, \dots, \alpha_A^{\text{age}}, \epsilon_{111}, \dots, \epsilon_{11A}, \epsilon_{121}, \dots, \epsilon_{12A}, \dots, \epsilon_{2TA} \right)^T,$$

$$\mathbf{m} = \left( m^{(1,1,1)}, \dots, m^{(1,1,A)}, m^{(1,2,1)}, \dots, m^{(1,2,A)}, \dots, m^{(2,T,A)} \right)^T.$$

It suffices to sample  $\boldsymbol{\eta} \mid \mathbf{Y}$ . The prior distribution of  $\boldsymbol{\eta}$  is  $N(\mathbf{0}, \boldsymbol{\Omega}^{-1})$ , where the prior precision matrix  $\boldsymbol{\Omega} = \text{bdiag}(\frac{1}{100}\mathbf{I}_2, \boldsymbol{\Omega}_1, \boldsymbol{\Omega}_2, \boldsymbol{\Omega}_3)$  is block diagonal with  $\boldsymbol{\Omega}_1, \boldsymbol{\Omega}_2$  and  $\boldsymbol{\Omega}_3$  being the corresponding prior precision matrices of the latent time effect, age effect, and independent noise terms.

Denote  $\mathbf{z} = (z^{(1,1,1)}, \dots, z^{(1,1,A)}, z^{(1,2,1)}, \dots, z^{(1,2,A)}, \dots, z^{(2,T,A)})$  with

$$z^{(s,t,a)} = \sum_{i=1}^{n_{sta}} Y_i \mid m^{(s[i],t[i],a[i])} \sim \text{Bin}(n_{sta}, \text{logit}^{-1}(m^{(s[i],t[i],a[i])}))$$

where  $n_{sta}$  denotes the sample size under sex  $s$ , time period  $t$  and age group  $a$ . We apply Pólya-Gamma augmentation and sample  $\boldsymbol{\eta}$  by introducing latent random variables  $\boldsymbol{\omega} = (\omega_1, \dots, \omega_{2TA})$ :

$$\omega_l \mid \boldsymbol{\eta} \sim PG(n_l, \mathbf{P}_l^T \boldsymbol{\eta}) \quad \text{for } l = 1, \dots, 2TA,$$

$$\boldsymbol{\eta} \mid \boldsymbol{\omega}, \mathbf{z} \sim MVN(\mathbf{M}, \mathbf{V})$$

where  $\mathbf{M} = \mathbf{V}\mathbf{P}^T(\mathbf{z} - \mathbf{n}/2)$  and  $\mathbf{V} = (\boldsymbol{\Sigma}^{-1} + \mathbf{P}^T \text{diag}(\boldsymbol{\omega})\mathbf{P})^{-1}$ .

4. Sample  $\phi_{ckj} \mid \mathbf{Y}, \mathbf{X}, \mathbf{Z}$ , for  $c = 0, 1, k = 1, \dots, K, j = 1, \dots, p$ , with

$$\phi_{ckj} \mid \mathbf{Y}, \mathbf{X}, \mathbf{Z} \sim \text{Beta} \left( a_\phi + \sum_{i=1}^n \mathbb{1}_{\{Y_i=c, Z_i=k, X_{ij}=1\}}, b_\phi + \sum_{i=1}^n \mathbb{1}_{\{Y_i=c, Z_i=k, X_{ij}=0\}} \right)$$

5. Sample  $V_{ck}^{(s,t,a)} \mid \mathbf{Z}, \mathbf{Y}, \omega^{(s,t,a)}$ , for  $c = 0, 1, k = 1, \dots, K-1, s = 1, 2, t = 1, \dots, T, a = 1, \dots, A$  with

$$V_{ck}^{(s,t,a)} \mid \mathbf{Z}, \mathbf{Y}, \omega \sim \text{Beta} \left( 1 + \sum_{i=1}^{n_{sta}} \mathbb{1}_{\{Z_i=k, Y_i=c\}}, \omega_c^{(s,t,a)} + \sum_{i=1}^{n_{sta}} \sum_{r=k+1}^K \mathbb{1}_{\{Z_i=r, Y_i=c\}} \right)$$

6. Sample  $\omega_c^{(s,t,a)} \mid V_{ck}^{(s,t,a)}$ , for  $c = 0, 1, s = 1, 2, t = 1, \dots, T, a = 1, \dots, A$  with

$$\omega_c^{(s,t,a)} \mid V_{ck}^{(s,t,a)} \sim \text{Gamma} \left( a_\omega + K - 1, b_\omega - \log \left( \prod_{k=1}^{K-1} (1 - V_{ck}^{(s,t,a)}) \right) \right)$$

7. Sample  $\sigma_{\text{time}}^2 \mid \boldsymbol{\alpha}^{\text{time}}, \sigma_{\text{age}}^2 \mid \boldsymbol{\alpha}^{\text{age}}$  with

For the Random Walk model,

$$\sigma_{\text{time}}^2 \mid \boldsymbol{\alpha}^{\text{time}} \sim \text{Inv-Gamma} \left( \frac{T-1}{2} + 0.5, \frac{\sum_{t=2}^T (\alpha_t^{\text{time}} - \alpha_{t-1}^{\text{time}})^2}{2} + 0.0009 \right)$$

$$\sigma_{\text{age}}^2 \mid \boldsymbol{\alpha}^{\text{age}} \sim \text{Inv-Gamma} \left( \frac{A-1}{2} + 0.5, \frac{\sum_{a=2}^A (\alpha_a^{\text{age}} - \alpha_{a-1}^{\text{age}})^2}{2} + 0.0009 \right)$$

For the Independent model,

$$\sigma_{\text{time}}^2 \mid \boldsymbol{\alpha}^{\text{time}} \sim \text{Inv-Gamma} \left( \frac{T}{2} + 0.5, \frac{\sum_{t=1}^T (\alpha_t^{\text{time}})^2}{2} + 0.0015 \right)$$



$$\sigma_{\text{age}}^2 \mid \boldsymbol{\alpha}^{\text{age}} \sim \text{Inv-Gamma} \left( \frac{A}{2} + 0.5, \frac{\sum_{a=1}^A (\alpha_a^{\text{age}})^2}{2} + 0.0015 \right)$$

8. Sample  $\sigma_{\epsilon}^2 \mid \boldsymbol{\epsilon}$  with

$$\sigma_{\epsilon}^2 \mid \boldsymbol{\epsilon} \sim \text{Inv-Gamma} \left( \frac{2 \times T \times A}{2} + 0.5, \frac{\sum_{s=1}^2 \sum_{t=1}^T \sum_{a=1}^A (\epsilon_{sta})^2}{2} + 0.5 \right)$$

## 4 Numerical results

### 4.1 Simulated data

We consider two types of verification mechanisms in the simulation study. In case (i), the verification process depends on observed symptoms and covariates  $X$  and  $D$ . In case (ii), the verification process also depends on the unobserved cause of death  $Y$ . In the first case, unbiased estimation of prevalence is possible as Assumption 1 is satisfied. In the second case, the verification process is not conditionally ignorable and can lead to bias in parameter estimation. This situation can arise in practice when the verification process depends on variables associated with the cause of death but is unavailable to the data analysts. More specifically,

$$p(L_i \mid X_i = \boldsymbol{x}, A_i = a, T_i = t, Y_i = y) = \text{logit}^{-1}(a_t^{\text{time}} + a_a^{\text{age}} + \boldsymbol{b}_{ta}^T \boldsymbol{x} + c_1 y + c_2 (1 - y))$$

where  $c_1 = c_2 = 0$  in case (i), and  $c_1 \sim \text{Unif}(-0.4, 0)$ ,  $c_2 = -c_1$  in case (ii). For the choice of the coefficients in the verification mechanism, we consider the more realistic situations where we under-sample time periods with more deaths and over-sample time periods with

fewer deaths. We also over-sample the first two and last two age groups to reflect situations where the mortality patterns of younger and elder groups are of greater interest. For the other symptoms, we allow them to be weakly associated with the selection probability in a time-varying fashion. Specifically, we let

$$\begin{aligned}\mathbf{a}^{\text{time}} &= [1.2, 0.1, \dots, 0.1, 1.2], \\ \mathbf{a}^{\text{age}} &= [0.4, 0.4, -1.6, \dots, -1.6, 0.4, 0.4], \\ b_{tj} &= 0.1 \mathbb{1}_{\{j \in \mathcal{S}_t\}}, \quad j = 1, \dots, p.\end{aligned}$$

where  $\mathcal{S}_t \subset \{1, \dots, p\}$  is a set of three randomly chosen indices for each time-level stratum. For the first and last two age groups, this leads to about 60% of deaths being verified in the middle of eight time periods and about 85% verified in the first and last time periods. For the other four age groups, this leads to about 20% of deaths being verified in the middle of eight time periods, and about 40% verified in the first and last time periods.

To mimic the true prevalence through time and age groups, we generate the true prevalence  $\pi_{sta}$  with the additive polynomial trend in both time and age dimensions. The simulated prevalence is shown as the black dots in Figure 5. The cause-of-death  $Y$  and symptoms  $X$  are generated according to the latent class model described in Section 2 with  $K = 10$ . We consider  $q = 10$ ,  $T = 10$ , and  $A = 8$ . The sample size for each sub-population is balanced with  $n_{sta} = 100$ . We generate 50 synthetic datasets and fit all models with  $K = 10$ .

We first illustrate the bias induced by not accounting for the verification process discussed in Section 2.1. Here we compare the four models stratified by sex, age, and time, with the unstratified baseline model described in Section 2.4. This baseline corresponds to the naive

adoption of VA cause-of-death assignment algorithms without considering the time-varying verification probability. It should be noted that the unstratified baseline model also includes the latent class model component and is more flexible than the VA models currently used in practice that assume conditional independence of symptoms McCormick et al. (2016); Byass et al. (2019). Since the unstratified model aims to estimate the overall prevalence in the population, we aggregate the estimated stratum-specific prevalence in the other four models to the population-level prevalence by

$$\hat{\pi} = \frac{1}{n} \sum_{s=1}^2 \sum_{t=1}^T \sum_{a=1}^A n_{sta} \hat{\pi}^{(s,t,a)}.$$

We take the posterior mean as our point estimates  $\hat{\pi}$  and evaluate the bias compared to the true prevalence,  $\hat{\pi} - \pi$ . Panel (a) of Figure 4 shows that the unstratified model leads to the largest bias across the simulated datasets in case (i). The three models with structured prior perform similarly and achieve much smaller bias compared to the unstructured model. Panel (c) of Figure 4 shows similar patterns for case (ii). It shows that the models that partially account for the verification process are also more robust when the conditional ignorability assumption is violated.

Next, we consider the bias from ignoring the heterogeneity of symptom distributions across strata, discussed in Sec 2.3. We consider the comparison between the models stratified by sex, age, and time, and simplified models stratified by time only. In the latter case, we include sex and age group as binary dummy variables in  $X$ , and remove the sex- and age-effect from the model for  $\pi$ . For the fully stratified model, we obtain the time-varying overall

prevalence using a similar aggregation step as before,

$$\hat{\pi}^{(t)} = \frac{\sum_{s=1}^2 \sum_{a=1}^A n_{sta} \hat{\pi}^{(s,t,a)}}{\sum_{s=1}^2 \sum_{a=1}^A n_{sta}}.$$

Panel (b) and (d) of Figure 4 compare the bias of  $\hat{\pi}^{(t)}$  based on the model with partial and full stratification, under the unstructured baseline and the random walk model. The fixed effect and models also show similar patterns. It can be observed that the fully stratified models are able to achieve consistently lower bias in both case (i) and (ii), due to its flexibility to incorporate stratum-specific symptom distribution.

Finally, we evaluate the effect of the structured prior on the stratum-specific prevalence estimates. Figure 5 illustrates the posterior means and 95% credible intervals for the prevalence estimates derived from a specific synthetic dataset in case (i). The unstructured baseline model yields prevalence estimates that exhibit notably higher variability over time and larger uncertainty. In contrast, the random walk model yields smoother estimates with narrower credible intervals, and generally captures the true value of prevalence more accurately.

## 4.2 Brazil COVID-19 surveillance data

We evaluate our methods on a flu syndrome surveillance dataset collected in Brazil from January to October, 2021. All deaths in this database had severe acute respiratory syndrome by COVID, other respiratory diseases or chronic diseases. The dataset contains the final cause of death for 411,491 deaths. We consider  $p = 14$  binary indicators for each death, including symptoms such as fever, vomiting, loss of taste and smell, etc. In our analysis,

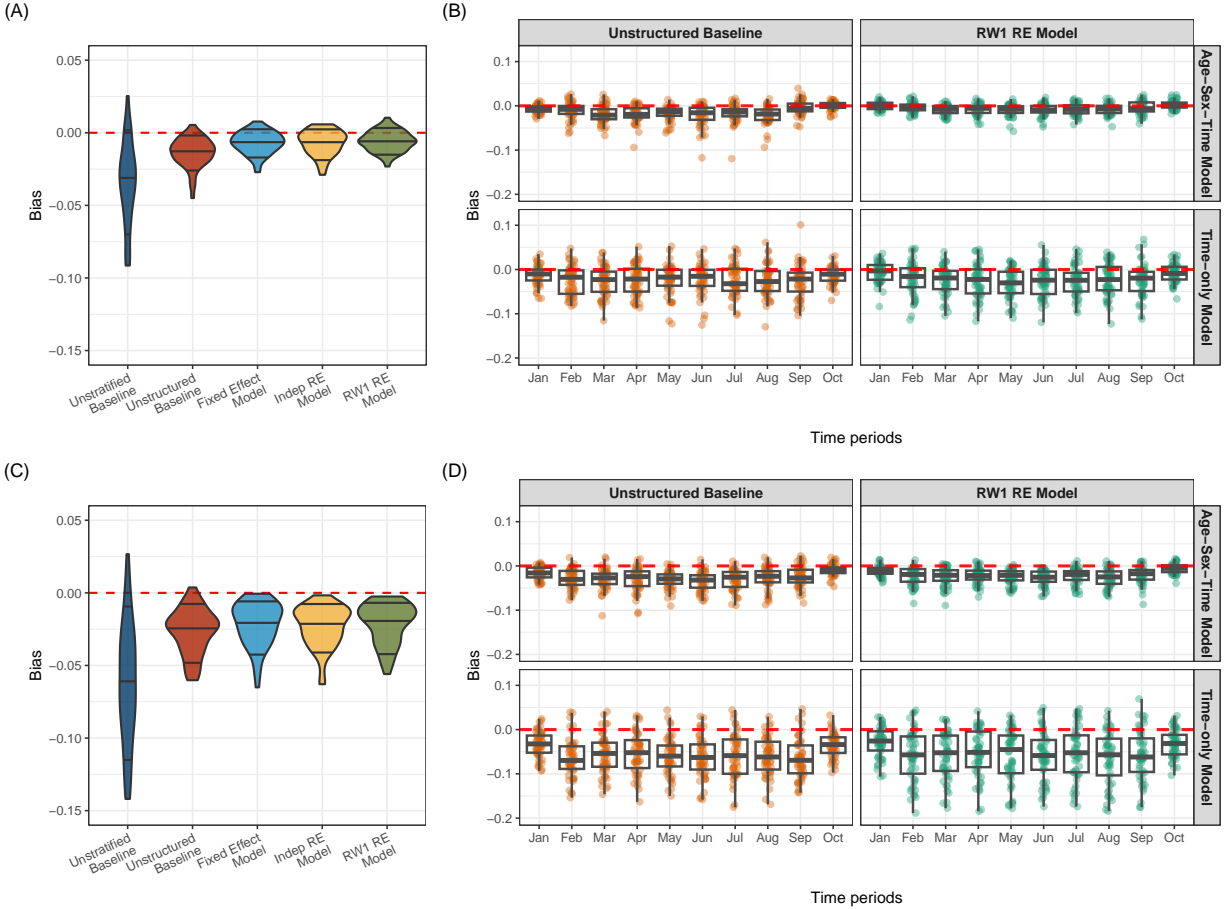


Figure 4: Bias of posterior mean prevalence estimates over 50 simulated datasets. The top row corresponds to simulation case (i) and the bottom row corresponds to simulation case (ii). Panel (A) and (C) evaluate the bias for population-level overall prevalence estimates and panel (B) and (D) evaluate the bias for time-varying overall prevalence estimates.

we exclude the information on vaccine, PCR and antigen test results as they are largely missing. Within this population of deaths suspected of COVID-19, the proportion of deaths with the final classification of being COVID-19 related increases from January to April and declines afterward. We consider eight age groups, where the first includes deaths between 0 and 30 years old and the subsequent groups are defined by ten-year increments. We let the first age group span 30 years because deaths under 20 years old are rare in this population. Figure 6 shows the true prevalence, i.e., the fraction of deaths due to COVID-19 among these

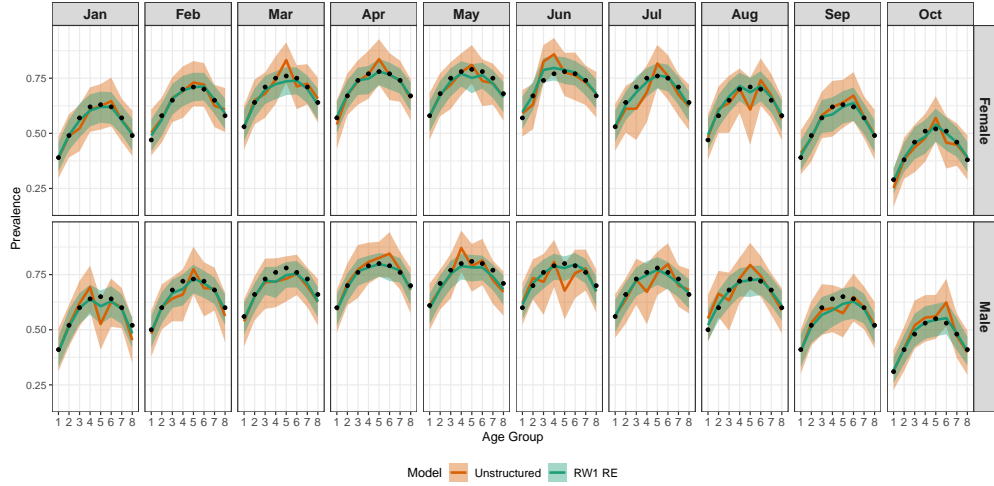


Figure 5: Posterior mean and 95% credible intervals of the estimated prevalence in one simulated dataset for different age groups, sex, and months. The true prevalence is indicated by the black dots.

suspected deaths, under each sub-population. The sex-specific trends differ from each other only mildly. Figure 7 illustrates that the sample sizes across sub-populations are notably imbalanced, with particularly small samples observed in January and October, as well as among the younger and elderly age groups.

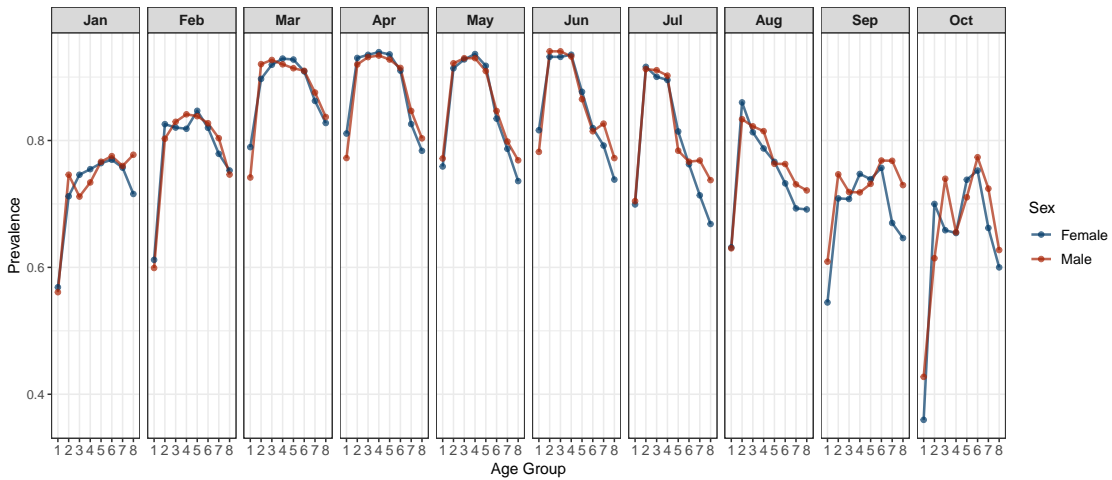


Figure 6: Fraction of deaths due to COVID-19 among the deaths suspected of COVID-19 across different age and sex strata over time.

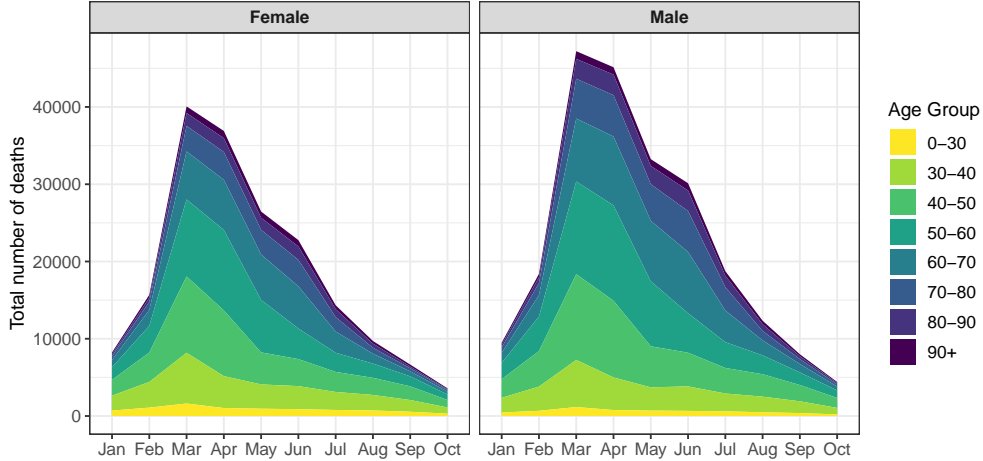


Figure 7: Total number of deaths in the COVID-19 surveillance dataset by age group, sex, and month.

We randomly sample 50% observations within each sex  $s$ , month  $t$  and age group  $a$ , while keeping the proportion of COVID-19 related death the same as the prevalence in the full population. We assume a verification mechanism that depends on time, age, and a random subset of symptoms, with the same coefficient as described in the simulation study,

$$p(L_i | X_i = \mathbf{x}, A_i = a, T_i = t) = \text{logit}^{-1}(a_t^{\text{time}} + a_a^{\text{age}} + \mathbf{b}_{ta}^T \mathbf{x}).$$

We generate 50 synthetic datasets and fit all models with  $K = 10$ . We run the MCMC for 8000 iterations with 3000 iterations as burn-in.

Figure 8 shows the posterior mean and 95% credible interval of the stratum-specific prevalence in one of the synthetic datasets, estimated by the four stratified models. Stronger effect of smoothing can be observed in the two random effect models, especially in the last two time periods when the total number of deaths is smaller.

To further compare the predictive performance of the four models, we compute the Con-

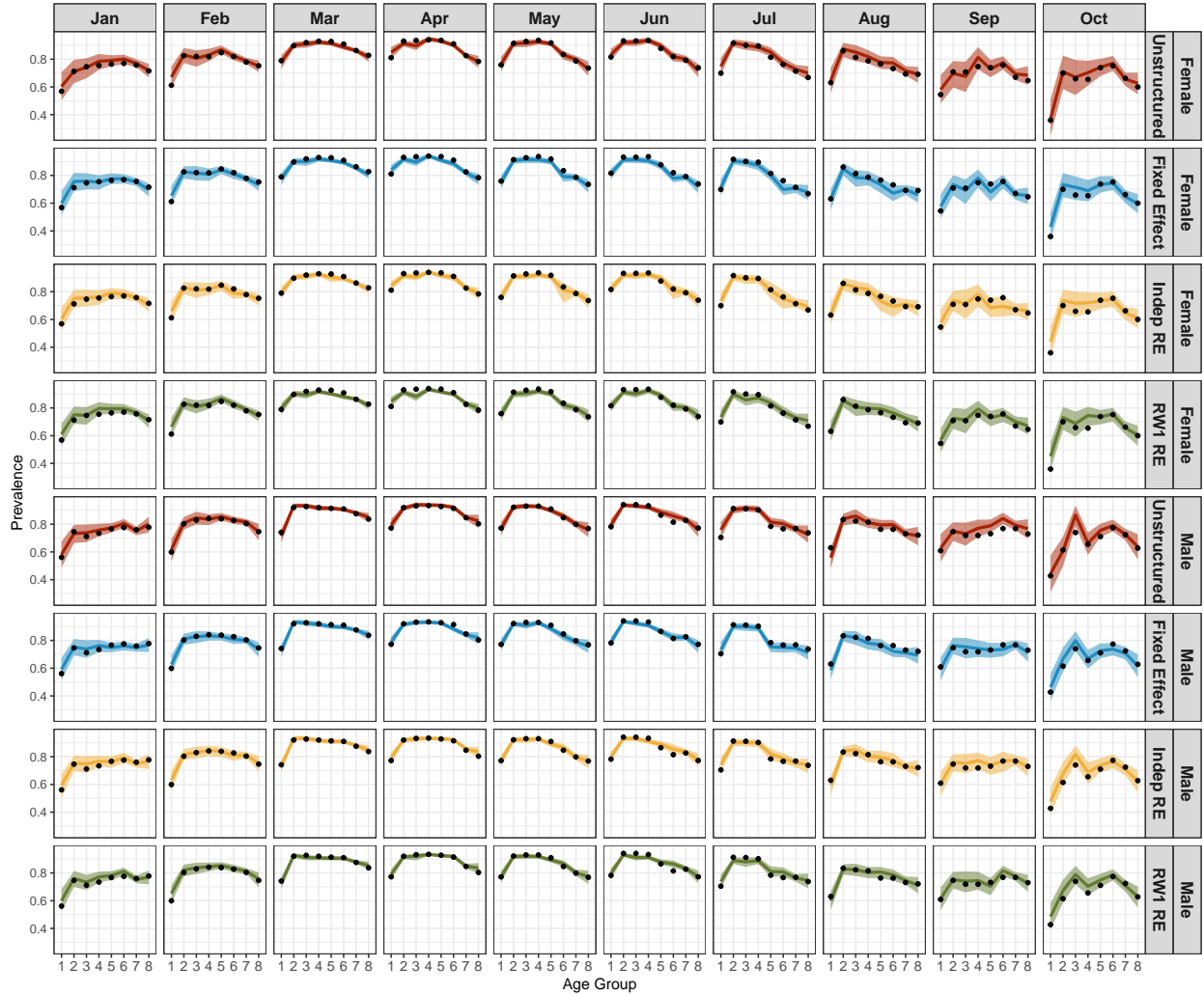


Figure 8: Posterior mean and 95% credible intervals of the estimated prevalence using the four models for different age group, sex, and months, based on one synthetic dataset resampled from the COVID-19 surveillance data from Brazil. The true prevalence is indicated by the black dots.

tinuous Ranked Probability Score (CRPS) (Gneiting and Raftery, 2007) for all four models.

CRPS is an extension of the squared error loss that takes into account the full predictive distribution instead of only a point estimate. For a probabilistic prediction distribution  $F$ ,



CRPS is defined as follows,

$$CRPS(F, x) = E_F |X - x| - \frac{1}{2} E_F |X - X'|.$$

where  $X \sim F$  and  $X' \sim F$  are two independent random variables, and  $x$  is the true prevalence. CRPS is positive, where values closer to 0 indicate better prediction. We compute the CRPS difference between the baseline and each of the three structured models. Positive differences indicate that the structured models outperform the baseline. Figure 9 shows the CRPS differences for the three models, compared to the unstructured baseline model, across all sub-populations in the 50 datasets. As expected, we can observe improved CRPS from all three structured models when the sample size is small and the proportion of unverified deaths is high.

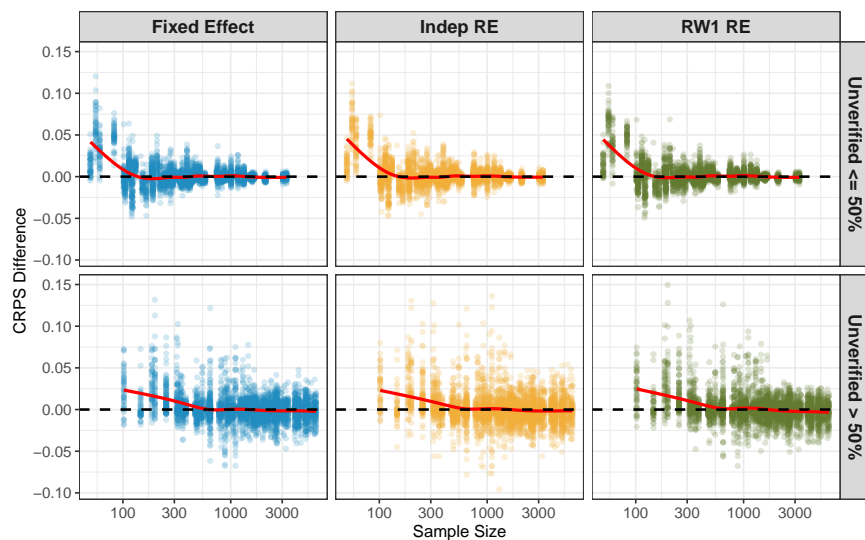


Figure 9: Improvement in CRPS compared to the unstructured baseline model for the three structured models, in terms of difference in CRPS. Each dot represents one sub-population in one simulated dataset, arranged by the sample size of the sub-population, and the proportion of unverified labels, i.e., the proportion of deaths without a cause, in the sub-population. The red line is the smoothed conditional mean for the points.

Figure 10 shows the similar pattern of bias as illustrated in the simulation study. The unstructured baseline model results in the largest bias for the population-level overall prevalence, due to not accounting for the time-varying verification mechanism. Figure 11 shows that for all models, accounting for the heterogeneity of symptom distributions over sex and age also greatly improves prevalence estimation.

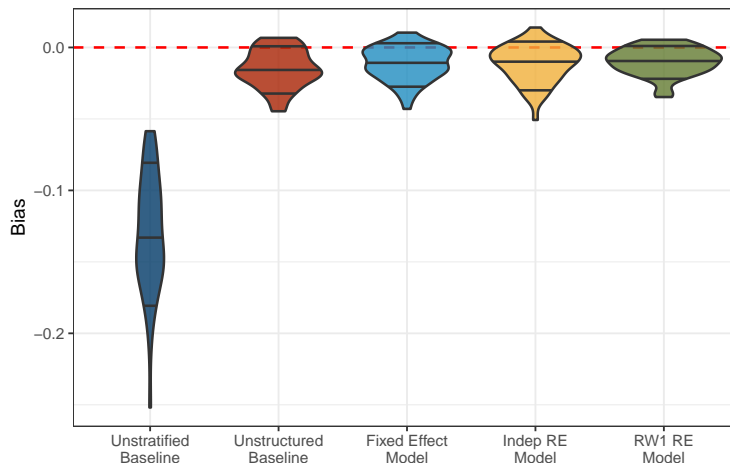


Figure 10: Distribution of bias of overall prevalence estimation over 50 synthetic datasets resampled from the COVID-19 surveillance data from Brazil, under the population-level model and the four stratified models.

Finally, the proposed latent class model framework also allows us to gain more insight into how the data distribution shifts over time by examining the estimated latent parameters. Figures 12 visualizes the heatmap of latent symptom profiles and the corresponding weights across different strata under the random walk model in one synthetic data. The latent classes are ordered by the expected number of symptoms under the symptom profiles of each class. We can observe distinct clusters of symptoms, such as fever and cough; dyspnea, respiratory discomfort, and low  $O_2$  saturation; loss of taste and loss of smell, that are more likely to occur in the same latent symptom profiles, which seem to correspond to symptoms with shared

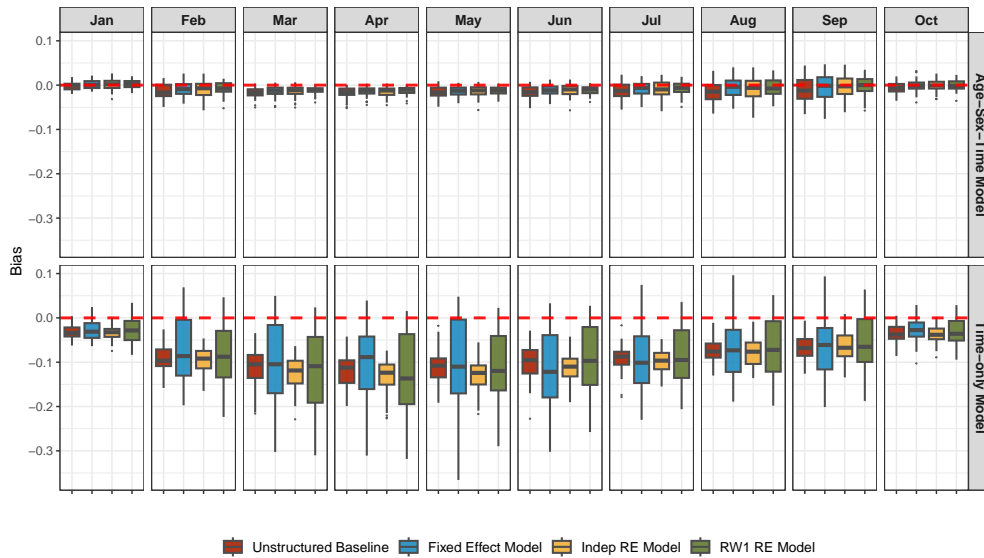


Figure 11: Bias of time-varying prevalence estimation over 50 synthetic datasets resampled from the COVID-19 surveillance data from Brazil, under the four models stratified by sex, age, and time (top row) and the models stratified by time only (bottom row).

mechanism. The estimated weights  $\lambda$  illustrate the changes in abundance of these latent classes over age, sex, and time. For example, among the deaths related to COVID-19, the weights of the fifth latent class are much larger in male deaths under 60 years old, compared to other demographic groups, whereas the sixth latent class has larger weights among deaths above 60 years old. Both symptom profiles include high probabilities of dyspnea, respiratory discomfort, and low  $O_2$  saturation. The main difference in these two latent symptom profiles is that the former includes higher probability of fever and cough, whereas the latter includes low probability of fever and cough, but higher probability of having at least one risk factors. These patterns are consistent with the explorative analysis in Figure 2.

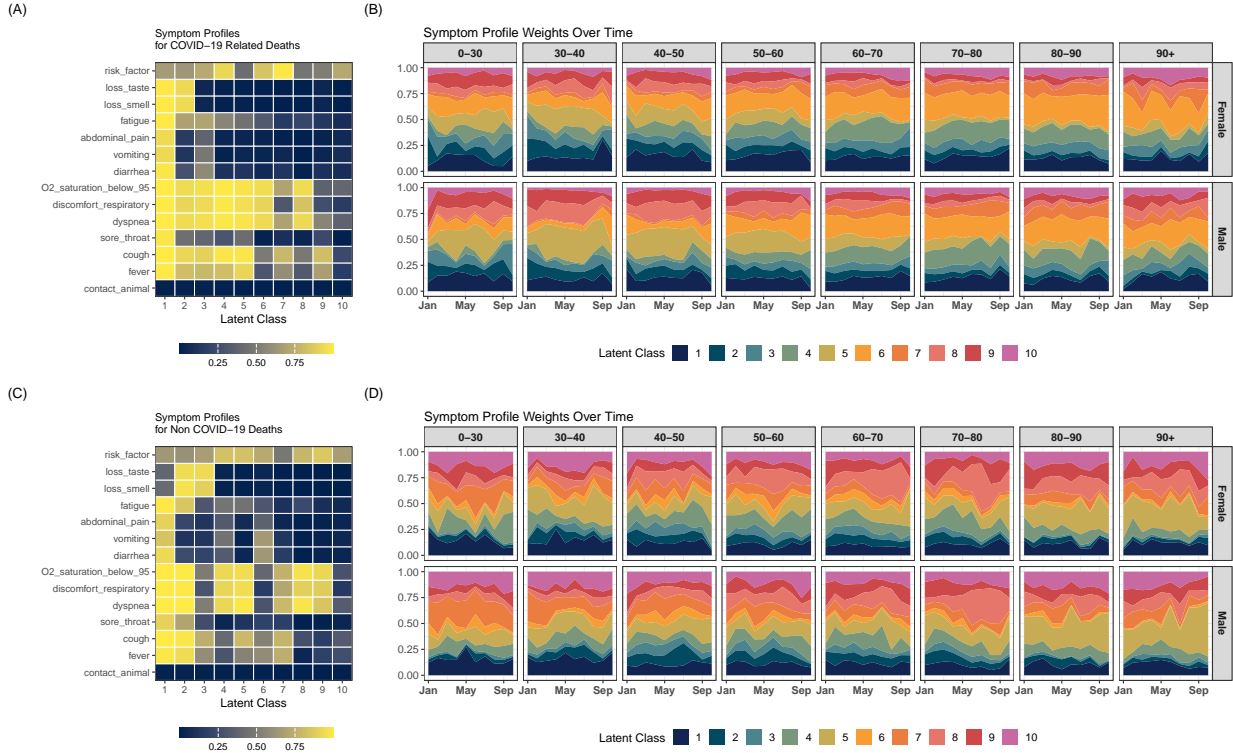


Figure 12: Posterior mean of latent parameters estimated in one synthetic dataset resampled from the COVID-19 surveillance data from Brazil. Panel (a): symptom profiles  $\phi$  by latent class for deaths related to COVID-19, ordered by the expected number of symptoms. Panel (b): latent class weights  $\lambda$  over sex, age, and time for deaths related to COVID-19. Panel (c) and (d) are the same parameters for deaths not related to COVID-19.

## 5 Discussion

In this paper, we introduce a hierarchical latent class model framework for modeling partially verified VA data and estimating the sub-population prevalence of a target cause of death. We describe conditions under which valid inference of the prevalence can be made and propose the novel use of structured priors to borrow information across sub-populations. We demonstrate that our model is able to avoid the bias induced by informative sampling of reference deaths and the structured priors can improve the robustness and interpretability of estimated prevalence.

There are several limitations of the proposed model. First, in the context of classifying COVID-19 deaths, information on PCR or antigen tests provides a key piece of information. However, the availability of tests needs to be taken into account and we generally should not treat it as missing at random. More generally, an important direction of future research is to deal with non-random missing indicators in both  $X_E$  and  $X_C$ . Second, we treat the latent class distribution to be independent a priori in the current model. When sample sizes are small, further incorporating structured priors on the latent class probabilities  $\lambda$  could further improve the estimation of the indicator distributions and may lead to better overall classification performance. Finally, existing VA algorithms largely take an overly simplified view on the causal structures among the collected indicators. While we have explored in this paper the role of two indicators, i.e., age and sex, as a stratification variable, more work is needed to further develop a more comprehensive framework to incorporate causal structures among all the collected indicators into the VA models, as such information could be key for proper generalizability of the algorithm across different populations.

## 6 Acknowledgments

We would like to thank Dr. Fatima Marinho and Dr. Luiz Fernando Ferraz for sharing the Brazilian COVID-19 surveillance data and helpful discussion of the results.

ZY and ZRL were supported by grant R03HD110962 from the Eunice Kennedy Shriver National Institute of Child Health and Human Development (NICHD), and in part by the Bill & Melinda Gates Foundation. The findings and conclusions contained within are those of the authors and do not necessarily reflect positions or policies of the Bill & Melinda Gates

Foundation.

## References

- Alert, G., Team, R., Organization, W. H., et al. (2003). Investigating cause of death during and outbreak of ebola virus haemorrhagic fever: draft verbal autopsy instrument. Technical report, World Health Organization.
- Byass, P., Hussain-Alkhateeb, L., D’Ambruoso, L., Clark, S., Davies, J., Fottrell, E., Bird, J., Kabudula, C., Tollman, S., Kahn, K., et al. (2019). An integrated approach to processing who-2016 verbal autopsy data: the interval-5 model. *BMC medicine*, 17(1):1–12.
- Chandramohan, D., Fottrell, E., Leitao, J., Nichols, E., Clark, S. J., Alsokhn, C., Cobos Munoz, D., AbouZahr, C., Di Pasquale, A., Mswia, R., et al. (2021). Estimating causes of death where there is no medical certification: evolution and state of the art of verbal autopsy. *Global Health Action*, 14(sup1):1982486.
- de Souza, P. M. M., Gerson, G., Dias, J. S., de Melo, D. N., de Souza, S. G., Ruiz, E. M., Fernandes Tavora, F. R., and Cavalcanti, L. P. d. G. (2020). Validation of verbal autopsy and nasopharyngeal swab collection for the investigation of deaths at home during the COVID-19 pandemics in Brazil. *PLOS Neglected Tropical Diseases*, 14(11):e0008830.
- Dunson, D. B. and Xing, C. (2009). Nonparametric bayes modeling of multivariate categorical data. *Journal of the American Statistical Association*, 104(487):1042–1051.
- Gao, Y., Kennedy, L., Simpson, D., and Gelman, A. (2021). Improving multilevel regression and poststratification with structured priors. *Bayesian analysis*, 16(3):719.

- Gneiting, T. and Raftery, A. E. (2007). Strictly proper scoring rules, prediction, and estimation. *Journal of the American statistical Association*, 102(477):359–378.
- King, G. and Lu, Y. (2008). Verbal autopsy methods with multiple causes of death. *Statistical Science*, 100(469).
- Kügelgen, J., Mey, A., Loog, M., and Schölkopf, B. (2020). Semi-supervised learning, causality, and the conditional cluster assumption. In *Conference on Uncertainty in Artificial Intelligence*, pages 1–10. PMLR.
- Kunihama, T., Li, Z. R., Clark, S. J., and McCormick, T. H. (2020). Bayesian factor models for probabilistic cause of death assessment with verbal autopsies. *The Annals of Applied Statistics*.
- Kunihama, T., Li, Z. R., Clark, S. J., and McCormick, T. H. (2024). Bayesian analysis of verbal autopsy data using factor models with age-and sex-dependent associations between symptoms. *arXiv preprint arXiv:2403.12288*.
- Li, Z. R., Thomas, J., Choi, E., McCormick, T. H., and Clark, S. J. (2023). The openva toolkit for verbal autopsies. *The R Journal*, page 1. <https://journal.r-project.org/articles/RJ-2023-020/>.
- Li, Z. R., Wu, Z., Chen, I., and Clark, S. J. (2024). Bayesian nested latent class models for cause-of-death assignment using verbal autopsies across multiple domains. *Annals of Applied Statistics*, 18(2):1137–1159.
- Maher, D., Biraro, S., Hosegood, V., Isingo, R., Lutalo, T., Mushati, P., Ngwira, B., Nyirenda, M., Todd, J., and Zaba, B. (2010). Translating global health research aims



- into action: the example of the alpha network. *Tropical Medicine & International Health*, 15(3):321–328.
- Matthews, B. W. (1975). Comparison of the predicted and observed secondary structure of t4 phage lysozyme. *Biochimica et biophysica acta*, 405 2:442–51.
- McCormick, T. H., Li, Z. R., Calvert, C., Crampin, A. C., Kahn, K., and Clark, S. J. (2016). Probabilistic cause-of-death assignment using verbal autopsies. *Journal of the American Statistical Association*, 111(515):1036–1049.
- Mercer, L. D., Wakefield, J., Pantazis, A., Lutambi, A. M., Masanja, H., and Clark, S. (2015). Space-time smoothing of complex survey data: small area estimation for child mortality. *The annals of applied statistics*, 9(4):1889.
- Moran, K. R., Turner, E. L., Dunson, D., and Herring, A. H. (2021). Bayesian hierarchical factor regression models to infer cause of death from verbal autopsy data. *Journal of the Royal Statistical Society: Series C (Applied Statistics)*.
- Nkengasong, J., Gudo, E., Macicame, I., Maunze, X., Amouzou, A., Banke, K., Dowell, S., and Jani, I. (2020). Improving birth and death data for african decision making. *The Lancet Global Health*, 8(1):e35–e36.
- Rao, J. N. and Molina, I. (2015). *Small area estimation*. John Wiley & Sons.
- Rosen, T., Safford, M. M., Sterling, M. R., Goyal, P., Patterson, M., Al Malouf, C., Ballin, M., Del Carmen, T., LoFaso, V. M., Raik, B. L., Custodio, I., Elman, A., Clark, S., and Lachs, M. S. (2021). Development of the verbal autopsy instrument for COVID-19 (VAIC). *Journal of General Internal Medicine*, 36(11):3522–3529.

- Rubin, D. B. (1976). Inference and missing data. *Biometrika*, 63(3):581–592.
- Saqib, M. A. N., Rafique, I., Bashir, S., and Salam, A. A. (2014). A retrospective analysis of dengue fever case management and frequency of co-morbidities associated with deaths. *BMC research notes*, 7(1):1–5.
- Schölkopf, B., Janzing, D., Peters, J., Sgouritsa, E., Zhang, K., and Mooij, J. (2012). On causal and anticausal learning. In *29th International Conference on Machine Learning (ICML 2012)*, pages 1255–1262. Omnipress.
- World Health Organization (2021). WHO civil registration and vital statistics strategic implementation plan 2021-2025.
- Wu, Z., Li, Z. R., Chen, I., and Li, M. (2024). Tree-informed Bayesian multi-source domain adaptation: cross-population probabilistic cause-of-death assignment using verbal autopsy. *Biostatistics*, page kxae005.
- Zhou, X.-H. (1998). Correcting for verification bias in studies of a diagnostic test’s accuracy. *Statistical methods in medical research*, 7(4):337–353.